

# How “Quantum” is the D-Wave Machine?

Seung Woo Shin<sup>\*</sup>, Graeme Smith<sup>†</sup>, John A. Smolin<sup>†</sup>, and Umesh Vazirani<sup>\*</sup>

<sup>\*</sup>*Computer Science division, UC Berkeley, USA.*

<sup>†</sup>*IBM T.J. Watson Research Center, Yorktown Heights, NY 10598, USA.*

## Abstract

Recently there has been intense interest in claims about the performance of the D-Wave machine. Scientifically the most interesting aspect was the claim in [7], based on extensive experiments, that the D-Wave machine exhibits large-scale quantum behavior. Their conclusion was based on the strong correlation of the input-output behavior of the D-Wave machine with a quantum model called simulated quantum annealing, in contrast to its poor correlation with two classical models: simulated annealing and classical spin dynamics. In this paper, we outline a simple new classical model, and show that on the same data it yields correlations with the D-Wave input-output behavior that are at least as good as those of simulated quantum annealing. Based on these results, we conclude that classical models for the D-Wave machine are not ruled out. Further analysis of the new model provides additional algorithmic insights into the nature of the problems being solved by the D-Wave machine.

## 1 Introduction

In a future world of quantum devices, it will become increasingly important to test that these devices behave according to specification. While this is clearly a central issue in the context of quantum cryptography [4, 27] and certified random number generators [17, 26], it is also quite fundamental in the context of testing whether a claimed quantum computer is really quantum [2, 18, 14, 5]. Recently, this last issue has featured prominently in the context of the D-Wave machine [12, 6, 7, 1, 15], amidst questions about whether it should really be thought of as a quantum computer and whether it provides speedups over classical computers. One of the grounds for skepticism is that the decoherence time of D-Wave’s qubits is reported to be on the order of nanoseconds, which is comparable to the time for a single operation and much shorter than the time required to carry out a computation, which is on the order of microseconds.

By now, claims about speedups over classical computers [16] have been largely refuted [7, 22, 19]. But one of the papers [7] that disproved the claims of quantum speedup

also claimed based on extensive experiments that the D-Wave machine exhibits large-scale quantum behavior. While falling far short of the existence of a working quantum computer, this conclusion is nonetheless very exciting, since it suggests that it might be possible to create large-scale entanglement without investing in stable, slowly decohering qubits. For this reason it is particularly important to closely examine the evidence presented in the paper.

The paper recorded the input-output behavior of the machine D-Wave One on a thousand randomly chosen inputs and compared it to the input-output behavior obtained by simulating three models. The first model was simulated quantum annealing<sup>1</sup>, and the other two were classical models — simulated annealing, and classical spin dynamics suggested in [23]. The paper reported that the input-output behavior of D-Wave One correlated highly with simulated quantum annealing, but despite considerable effort in choosing parameters did not correlate well with the two classical models. Based on this, the paper concluded that the D-Wave machine was indeed following quantum dynamics, and exhibited large-scale quantum behavior.

At a high level, the nature of this argument is very interesting, and reminiscent of the algorithmic approaches in [2, 18, 9, 14, 5]. In those papers, the quantum system to be tested is modeled as a black box, and elaborate protocols are designed whose execution guarantees that the untrusted quantum systems behaves according to specification. Given the limited access to the D-Wave machine, which is proprietary and with access controlled by the company, the approach of [7] may be seen as algorithmic in nature. The evidence of “quantumness” is based on broad algorithmic differences between the three models rather than detailed physical modeling of the system. In particular, the core of the argument is based on the finding that the D-Wave machine and simulated quantum annealing generally find the same set of instances to be “hard” and the same set of instances to be “easy.” The hardness of an instance is measured by the number of times that each candidate algorithm succeeds in finding the optimal solution out of one thousand trials. Of course, how convincing this evidence is depends upon how comprehensive the list of candidate classical models is.

In this paper, we consider a third classical model for the D-Wave machine. The model is quite natural, and it replaces each spin in the D-Wave machine with a magnet pointing in some direction in the XZ plane. Each magnet is subject to both an external magnetic field as well as dipole-dipole couplings due to interactions with nearest neighbors on the so-called Chimera graph. The external magnetic field is attenuated at the same rate as in [8], while the couplings between magnets also follow the schedule from [8]<sup>2</sup>. We consider

---

<sup>1</sup>Simulated quantum annealing refers to a quantum Monte Carlo simulation of quantum annealing. In this sense, it is a classical algorithm. However, one can argue that the quantum Monte Carlo simulation is quite involved and the D-Wave machine is surely not carrying out such a complex computation. Therefore, it may be reasonable to regard this as a quantum process.

<sup>2</sup>We note that the schedule we consider here is different from the one reported in [7]. We were informed [24] that the schedule in [7] was based on an error by D-Wave, and the correct schedule is reported

the input-output behavior of this model on the same set of one thousand inputs. Our simulations show that it achieves as good or better correlation with the D-Wave machine’s input-output behavior than simulated quantum annealing does. Based on these results, it is safe to say that classical models for the D-Wave machine are not ruled out, and it is premature to conclude that the D-Wave machine exhibits large-scale quantum behavior.

Matthias Troyer suggested [24] a direct comparison between our model and simulated quantum annealing, which reveals an extremely high correlation of  $R \approx 0.99$  (Fig 9). One way to view this result is that our model is the classical analogue of a mean-field approximation to simulated quantum annealing, and that for the set of problems solved by D-Wave One, this approximation is very accurate. This helps explain why the correlation of the D-Wave data with simulated quantum annealing does not preclude a classical model for D-Wave.

Further analysis of the algorithmic behavior of this new model also provides new insights into the nature of the computational problem being solved, namely the problem of finding the ground state of a classical Ising spin glass on the so-called Chimera graphs. The Chimera graph consists of super-nodes or clusters of 8 qubits (connected in a complete bipartite graph  $K_{4,4}$ ) arranged in a two-dimensional grid. The D-Wave machine consists of superconducting qubits arranged on the vertices of such a graph, with a  $z - z$  coupling between neighboring qubits. An analysis of the new model suggests that the existence of these super-nodes greatly reduces the effective size of the computational problem being solved, so that heuristically the size of the problem should be thought of as the number of super-nodes  $m = 16$ , rather than the number of qubits  $n = 108$ . To the extent that the model accurately represents the dynamics of the D-Wave machine, it therefore has great implications for the performance of the D-Wave machine as it is scaled up to larger numbers of qubits.

## 2 Background

We start by defining the computational problem that D-Wave machines are designed to solve. The “native” problem of D-Wave machines is the problem of finding the ground state of a classical Ising spin glass, which can be described as follows. The input to the problem is a weighted graph with  $n$  vertices, where each vertex represents a spin and each edge represents interaction between the two incident vertices. The edge weights  $J_{ij}$  can be either 1 or  $-1$ , corresponding to ferromagnetic and antiferromagnetic interaction respectively. The problem is simply to assign a spin value  $z_i \in \{-1, 1\}$  to each vertex  $i$  so that the energy  $H = -\sum_{i<j} J_{ij} z_i z_j$  is minimized, i.e. finding the “ground state” of the given interaction graph.

An additional constraint imposed by D-Wave machines is that the input graph must be a

---

in [8]. Our results are reported for this new schedule. All the claims we report here apply equally well to the previous schedule in [7].

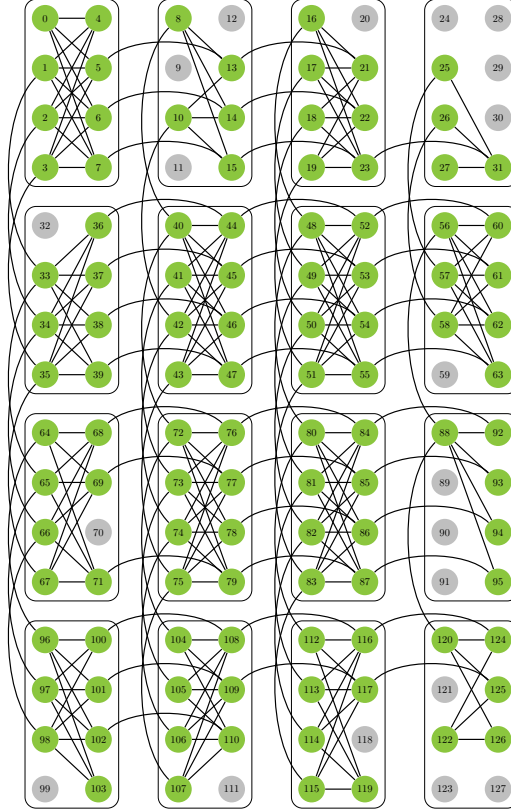


Figure 1: The “Chimera” graph structure implemented by the D-Wave One. Grey dots represent the twenty non-working qubits in the D-Wave One. Figure is from [7].

subgraph of the so-called Chimera graph, which is depicted in Figure 1. The Chimera graph consists of copies of complete bipartite graphs  $K_{4,4}$ ’s which are laid out in 2D lattice as in Figure 1. We will refer to each copy of  $K_{4,4}$  as “supernode.” Note that the left qubits in each supernode are coupled vertically in the 2D lattice and the right qubits horizontally. More specifically, each left qubit is coupled with the corresponding left qubit in the supernodes immediately above and below it, and each right qubit to the corresponding right qubits in supernodes immediately to the right and left. On the coarser level, this structure can be viewed as a 2D lattice of size  $4 \times 4$ . While the problem of finding the ground state of a classical Ising spin glass is NP-hard, it is known to have a polynomial time approximation scheme when the input graph is a Chimera graph [20].

The D-Wave machine places a superconducting flux qubit at each node of the Chimera

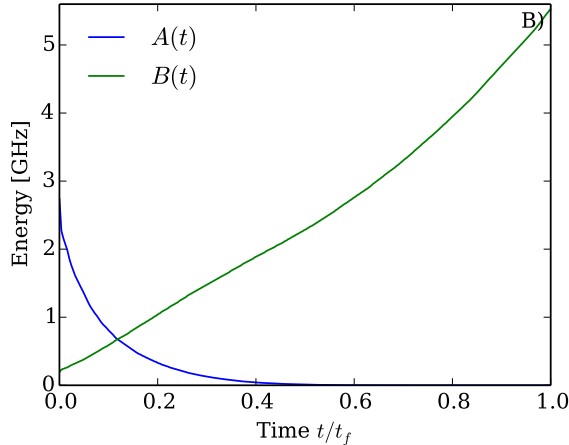


Figure 2: The annealing schedule of the D-Wave One. Figure is from [8].

graph. The time-dependent Hamiltonian of D-Wave machines is given by

$$H(t) = -A(t) \sum_{1 \leq i \leq n} \sigma_i^x - B(t) \sum_{i < j} J_{ij} \sigma_i^z \sigma_j^z$$

where  $A(t)$  and  $B(t)$  represent the “annealing schedule” of the machine, which is shown in Figure 2, and the process is carried out at a finite temperature. As mentioned in a footnote in the introduction, this schedule is different from the one reported in [7], which was based on an error by D-Wave [24], although this did not change their conclusions. Our paper is based entirely on the new corrected schedule [8]. We note that our conclusions also hold equally well for both schedules.

If the entire process were carried out sufficiently slowly and at zero temperature, then it would be an implementation of adiabatic quantum optimization [13]. Such a process is guaranteed to end up in the ground state of the target Hamiltonian  $H = -\sum_{i < j} J_{ij} Z_i Z_j$ . For this to happen, the total time for the process has to scale as  $\Omega(1/\Delta^2)$ , where  $\Delta$  is the minimum spectral gap of the time-dependent Hamiltonian where the minimum is taken over the annealing schedule. It is known that in the worst case  $\Delta$  scales exponentially in the problem size [13, 25, 3]. Quantum annealing can be thought of as a noisy version of adiabatic quantum computing which is carried out at a finite temperature.

Finally, we summarize the previous results on the question of whether D-Wave machines exhibit large-scale quantum behavior. We note that there were a few earlier papers that studied related questions [12, 6], but the first paper to study this question at a sufficiently large scale was [7], in which the behavior of the 108-qubit D-Wave One was compared to simulations of quantum and classical models. The method of comparison was as follows. First, one thousand instances of the Ising spin glass problem were generated randomly.

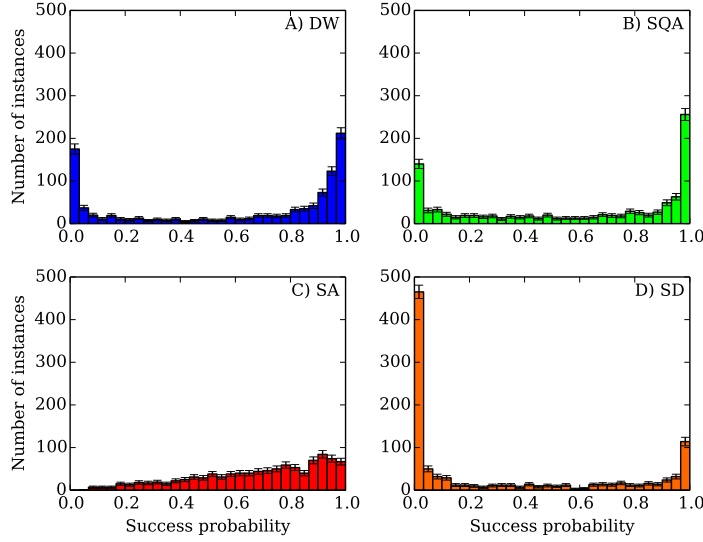


Figure 3: Histogram of success probabilities from [8]. It is observed that the histogram is bimodal for D-Wave, simulated quantum annealing, and classical spin dynamics, whereas it is unimodal for SA. This means that the former three algorithms divide the problem instances into two groups, namely “easy” and “hard.” They succeed almost always on the “easy” instances and fail almost always on the “hard” instances.

The problem size was 108 for all of these instances, in order that all of the 108 working qubits of the D-Wave One are utilized. Then, each of the following three algorithms were run one thousand times on each of these one thousand problem instances: the D-Wave One, simulated quantum annealing, and simulated (classical) annealing. Based on this, the success probability of each algorithm was recorded for each instance, where success is defined to be the finding of the exact optimum, i.e. the ground state, for the instance. The histogram of success probabilities of each algorithm, shown in Figure 3, served as the main evidence for the paper’s conclusion, which was that the D-Wave One was consistent with simulated quantum annealing rather than the classical models and therefore D-Wave One is indeed performing quantum annealing. A parallel conclusion of the paper was that their simulated annealing code was in fact up to 6 times faster than the D-Wave One, indicating no speedup over classical computers.

This result was immediately questioned by Smolin and Smith in [23], who pointed out that the unimodal histogram of simulated annealing was simply a consequence of statistical independence between different runs and that it was not a signature of all classical algorithms. They went on to propose a classical model for the D-Wave machine based on  $O(2)$  rotor model, which also exhibited bimodal signature in the success probability histogram.

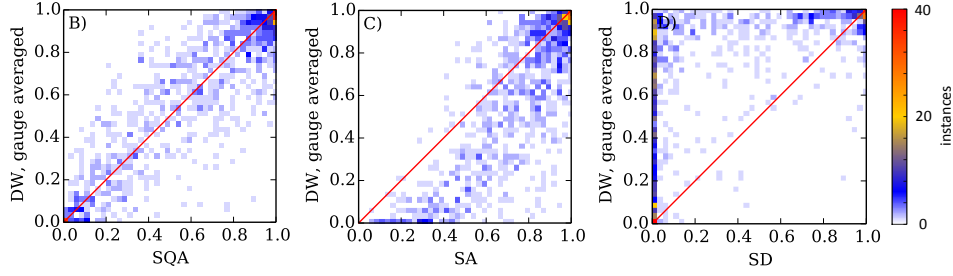


Figure 4: Scatterplot of success probabilities from [8]. The correlation between D-Wave and SQA is noticeably better than that between D-Wave and the classical models.

The authors of [7] soon responded in [28] that their conclusions were in fact based on more detailed correlation analysis, showing that the correlation between the D-Wave success probabilities and SQA success probabilities is much higher than the correlation between the D-Wave success probabilities and success probabilities of the classical models (Figure 4). Along with these results, they also released the dataset from their experiments as a service to the community, which allowed us to perform the study reported in this paper.

### 3 Results

In this paper, we consider the following classical model: each spin  $i$  is modeled by a classical magnet pointing in some direction  $\theta_i$  in the XZ plane (since there is no  $\sigma^y$  term in our time-dependent Hamiltonian, we can assume that there is no Y component). We assume that the angle  $\theta_i$  is measured in relation to  $\hat{x}$ . We further assume that there is an external magnetic field of intensity  $A(t)$  pointing in the  $\hat{x}$ -direction, and that neighboring magnets are coupled via either ferromagnetic or anti-ferromagnetic coupling, according to the specification of the input graph. Our Hamiltonian can then be rewritten as follows:

$$H(t) = -A(t) \sum_{1 \leq i \leq n} \cos \theta_i - B(t) \sum_{i < j} J_{ij} \sin \theta_i \sin \theta_j.$$

Thus, in the absence of noise, i.e. at zero temperature, each spin  $i$  will simply align with the net effective field at that location which is given by  $A(t)\hat{x} + B(t)\hat{z} \sum_j J_{ij} \sin \theta_j$ .

To model the noise in the system, we perform a Metropolis-type update inside this model. That is, at each time step, we do the following:

1. For each spin  $i$ , pick  $\theta'_i$  at random and compute the change in energy that would result if the spin were to change its state to  $\theta'_i$ :

$$\Delta E_i = -A(t)(\cos \theta'_i - \cos \theta_i) - B(t) \sum_j J_{ij} \sin \theta_j (\sin \theta'_i - \sin \theta_i)$$

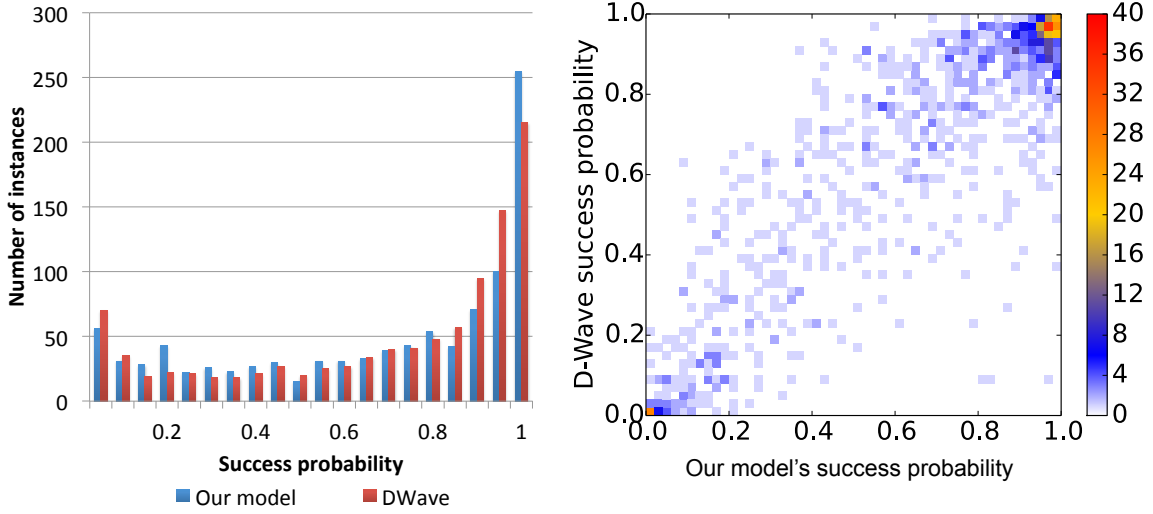


Figure 5: Histogram and scatterplot of our classical model. The correlation coefficient  $R$  between the D-Wave One and our model is about 0.89.

2. Update spin  $i$ 's state to  $\theta'_i$  with probability  $e^{-\Delta E_i/T}$  where  $T$  is the temperature of the system which is kept constant through the simulation.

Note that this model is related to the  $O(2)$  rotor model of [23], but differs in that we perform Metropolis-type updates instead of integrating the equation of motion. Indeed the update procedure is the direct analogue of the Metropolis algorithm in  $O(2)$  model.

Our experimental results (Figure 5) show that this simple model not only exhibits a bimodal signature similar to that of the D-Wave One or simulated quantum annealing, but it also achieves a very high correlation with the success probabilities of the D-Wave One which were published in [28]. Our success probabilities were obtained by simulating the above model one thousand times on each instance, where each run consisted of 500,000 steps and the system temperature was fixed at  $T = 0.22$ . We note that the correlation of 0.89 achieved by our model is higher than the correlation achieved by simulated quantum annealing in [8].

## 4 Discussion

It is instructive to analyze the behavior of our classical model and to compare and contrast it with simulated annealing. First, if the transverse field were set to 0, i.e. if  $A(t) = 0$  for all  $t$ , then the model simplifies to an  $O(2)$  analogue of simulated annealing. To see this, note that for the Metropolis acceptance probability function  $e^{-\Delta E_i/T}$ , keeping the temperature  $T$  constant and increasing the coupling strength  $B(t)$  has the same effect as keeping  $B(t)$  constant and decreasing the temperature  $T$  over time. Simple experiments confirm that



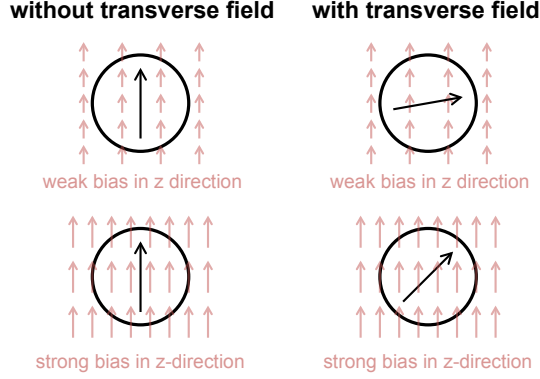


Figure 6: Role of transverse field

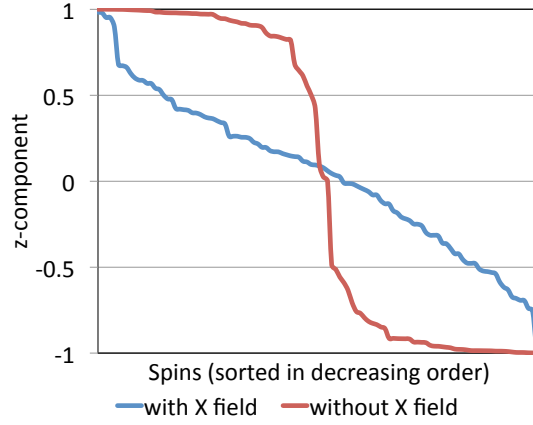


Figure 7: Snapshot of a typical run:  $z$ -components of the spins, sorted in decreasing order.

our model indeed exhibits a unimodal signature if the transverse field is removed. This indicates that the transverse field is the very source of bimodal signature.

To understand this better, a closer look at the model shows that an important effect of transverse field is to provide gradation in the magnitude of  $z$ -components of spins. Figure 6 schematically illustrates typical states of spins with and without transverse field. Note that in the absence of transverse field, each spin will simply align in the direction of the  $z$ -component of the net field at that location. That is, the spin will want to point completely up or completely down regardless of the actual strength of the field, as this is the configuration that minimizes energy. The presence of a transverse field completely alters this phenomenon, because the relative strengths of the  $z$ - and  $x$ - components determine the preferred direction of the spin.

Figure 7, in which we take a snapshot of a typical simulation and plot  $z$ -components of the spins, confirms that the above intuition is true. The values of  $z$ -components are concentrated around 1 and  $-1$  when there is no transverse field (red line), whereas they are more evenly distributed when there is transverse field (blue line). From an algorithmic viewpoint, it is worth drawing an analogy to spectral graph theory, in particular to the relationship between cuts and eigenvectors of graphs. In spectral graph theory, a cut of a graph is represented by a  $\{-1, 1\}$ -valued vector, while entries of an eigenvector of a graph can take on arbitrary real values. It is a well known fact that there exists a very interesting relationship between the two, which allows us to find a sparse cut in a given graph using information about its eigenvectors [11].

Why does the transverse field cause the model to behave more deterministically? Here we make the observation that a simulation of our model can be viewed as a fixed point iteration procedure which traces the equilibria of the time-dependent Hamiltonian. Note that there is a unique equilibrium at  $t = 0$ , namely the configuration where every spin points in the  $x$  direction. In fact, it is straightforward to prove that under the annealing schedule of Figure 2 and the assumption that the underlying interaction graph is a subgraph of the Chimera graph,  $H(t)$  has a unique equilibrium when  $t < 0.02$ . Moreover, we can invoke a theorem in topology [10, 21] to prove that all later equilibria are reachable from this unique equilibrium.

If we set the noise term in our model to 0, the evolution of the system is completely deterministic and therefore the same equilibrium will be reached on each run. In this case, simulation results are similar to that of [23] and it fails on too many instances to correlate well with the D-Wave machine. When there is noise, however, different equilibria are reached with different probabilities. Interestingly, our results (Figure 5) show that success probabilities are greatly enhanced with the introduction of noise. To obtain an intuitive understanding of this phenomenon, we designed the following experiment:

1. Up to  $t = t_{\text{thres}}$ , simulate our model as usual, with noise.
2. At  $t = t_{\text{thres}}$ , equilibrate the system under  $H(t_{\text{thres}})$ .
3. Resume the original simulation from  $t = t_{\text{thres}}$ , but with the transverse field  $A(t)$  completely turned off.

Remarkably, we were able to obtain a very high correlation of  $R \approx 0.99$  between our original model and this modified model using  $t_{\text{thres}} = 0.15$ . (The correlation with D-Wave One remained at about 0.88.) This result suggests the following picture for our model. In the first part of the evolution, i.e. when  $t < 0.15$ , we can understand the system to be making a probabilistic choice of one of the equilibria of  $H(t_{\text{thres}})$ . The probability with which each equilibrium is reached is governed by the behavior of the noise model. On the other hand, the second part of the evolution, i.e. when  $t > 0.15$ , can be understood as simulated annealing that begins at an effective temperature  $T/B(t)$  which is already quite low. This means that it can roughly be thought of as local search with small perturbations which explores a very small neighborhood of the given state. Therefore, this algorithm will

succeed if and only if the first part of the evolution brings the system into a state which is sufficiently close to the global optimum.

Another result of our simulations was that the number of different equilibria reached in the first part of the process was often surprisingly low. Averaged across all instances, we only saw 20.2 distinct equilibria at  $t = 0.15$ , which indicates that the size of the state space explored in the first part of the evolution is not comparable with our usual expectations for a problem of size  $n = 108$ . Moreover, in most cases we found that there existed a few equilibria that were strongly preferred to the others, making the state space even smaller in effect and the process more deterministic. Together with the picture suggested in the previous paragraph, this offers an approximate high-level explanation of the bimodal behavior of our model.

An interesting question that remains to be studied is what happens at the so-called “branching points,” namely at those values of  $t$  where the number of equilibria of  $H(t)$  jumps from 1 to 2, 2 to 3, and so on. In other words, what choices are being made at those branching points and in what ways do distinct “branches” differ? A case study on the instance 13-55-29 offers a very interesting insight into this question. The instance has two distinct equilibria at  $t = 0.054$ , up to the two-fold symmetry of  $z$ -flips of all spins. Figure 8 shows how the two equilibria differ from each other. The figure suggests that the choice being made at this particular branching point is the orientation between the “white” cluster and the “black” cluster. Note that if a wrong branch is selected here, the second part of the process will not be able to correct it, as it will have to flip the entire black cluster. This is because as we already saw, the second part of the process may be thought of as simulated annealing at low temperature, and in this case the number of spins that have to be flipped simultaneously is too large.

Similar analysis on other instances and other values of  $t$  confirms this intuition; branching points always correspond to points at which the orientation between large clusters gets determined. Moreover, as  $t$  increases, we see smaller and smaller clusters become involved in the process. That is, we eventually see branching points which determine the orientation between one or two supernodes and the rest of the spins. From an algorithmic viewpoint, this phenomenon has significant implications. Namely, it indicates that supernodes with highly stable local configurations get fixed early in the process, and therefore the main challenge in finding the global optimum lies in breaking their two-fold symmetry based on interaction with other supernodes. Note that the energy contribution from interactions within a particular supernode remains unchanged if every spin in the supernode is flipped. However, the energy contribution from interactions between supernodes depends crucially on the relative orientation between those supernodes.

Since simulated annealing performed in the second part of the process is not able to correct more than a handful of spins at once, the main difficulty of the problem lies in choosing a correct branch in the first part of the process. However, we have seen that different branches roughly correspond to different choice of orientation between supernodes. This observation has an important implication for the computational problem being solved,

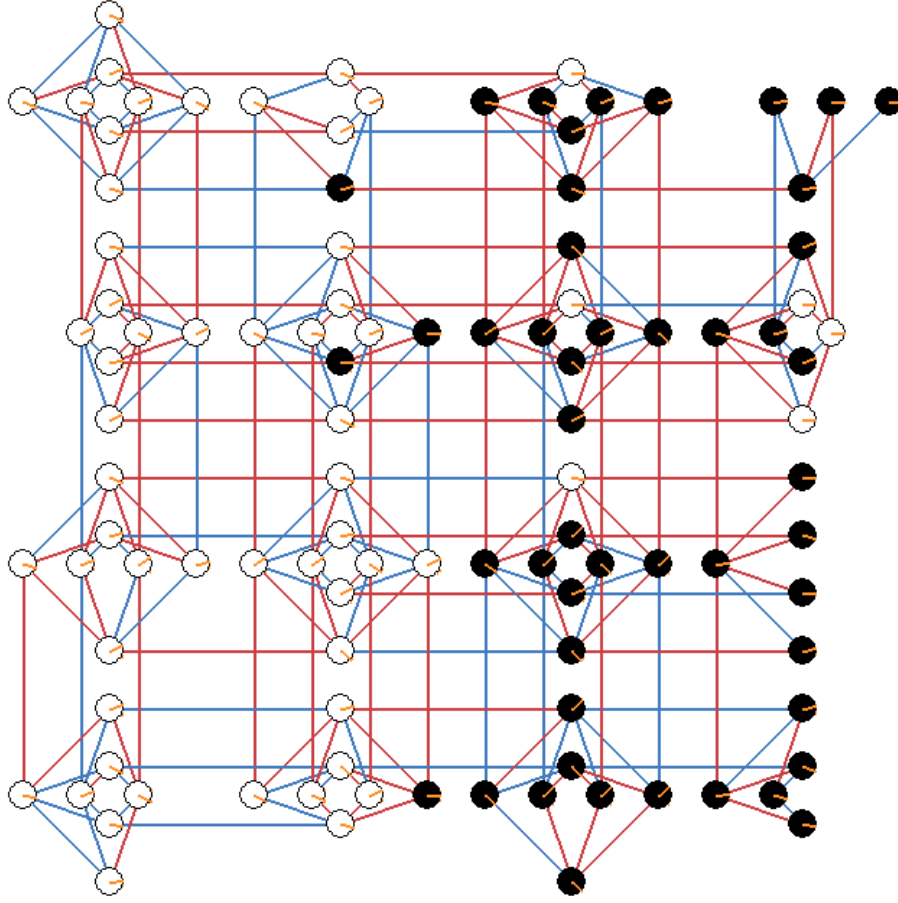


Figure 8: “Branching” of equilibria (Instance 13-55-29,  $t = 0.054$ ). Black dots indicate spins for which the sign of  $z$ -components differ between the two “branches.” Figure shows the less frequent of the two branches. Blue edge indicates ferromagnetic interaction and red edge antiferromagnetic interaction.

because it provides a sense in which the effective problem size may be thought of as closer to the number of supernodes  $m = 16$  rather than the number of spins  $n = 108$ . This could be one explanation of the fact that heuristic methods such as simulated annealing perform rather well on this type of problems despite the large problem size. Therefore, to the extent that our classical model accurately represents the dynamics of the D-Wave machine, it is reasonable to conjecture that the D-Wave machine, as well as any other heuristic method, will fail to solve these problems effectively when the number of supernodes  $m$  becomes sufficiently large.

It is worth emphasizing that the goal of this paper is not to provide a classical model

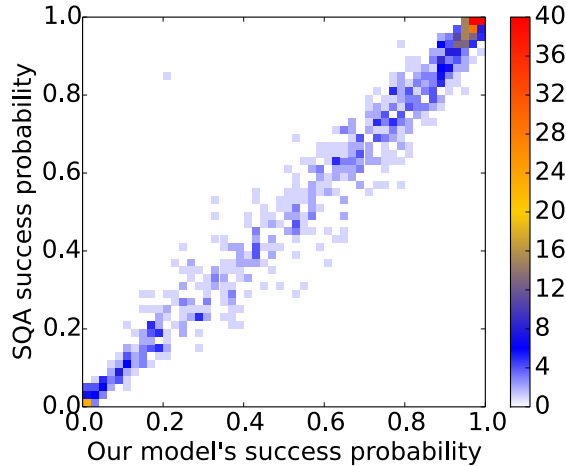


Figure 9: Correlation between simulated quantum annealing of [8] and our classical model. The correlation coefficient  $R$  is about 0.99.

for the D-Wave machine, but rather to critically examine the claim that there is no simple local classical model that correlates with its input-output behavior. The classical model introduced here is useful for the purposes of studying the large-scale algorithmic features of the D-Wave machine. The task of finding an accurate model for the D-Wave machine (classical, quantum or otherwise), would be better pursued with direct access, not only to programming the D-Wave machine, but also to its actual hardware.

## 5 Conclusions

This paper examined the interesting claims from a recent paper by [7] based on extensive experiments, that the 108 qubit D-Wave One machine exhibits large-scale quantum behavior. The nature of the argument in that paper is algorithmic: a strong correlation was observed between the input-output behavior of the D-Wave machine with a quantum model called quantum simulated annealing, whereas it correlated poorly with two classical models: simulated annealing and classical spin dynamics. In this paper, we suggest a simple classical model, which treats each spin in the D-Wave machine as a classical magnet, which couples to neighboring magnets as well as an external field. The evolution of the system proceeds according to a Metropolis-type dynamics. Simulation of this model on the same instances reported in [7] yields higher correlation with the D-Wave input-output behavior than those of simulated quantum annealing. One way to view our model is as a classical mean field approximation to simulated quantum annealing. A direct comparison between our model and simulated quantum annealing [24] reveals an extremely high correlation of  $R \approx 0.99$  (Fig 9). Hence, the correlation of the D-Wave data with simulated

quantum annealing does not impose any barrier to a classical model for D-Wave.

Further analysis of the new model indicates that the dynamics do not exhibit the kind of combinatorial explosion one might expect from a 108-bit problem. The reason appears to be related to the 8-bit clusters in the interaction graph that appear to have the effect of reducing the effective problem size to 16 rather than 108. To the extent that this model captures the essential algorithmic features of the D-Wave One machine, this suggests that scaling to machines with larger numbers of qubits should lead to increasing problems with combinatorial explosion.

## Acknowledgments

SWS and UV were supported by ARO Grant W911NF-09-1-0440 and NSF Grant CCF-0905626. We thank Matthias Troyer, Sergio Boixo, and Troels F. Rønnow for useful discussions and for sharing their unpublished experimental data with us.

## References

- [1] S. Aaronson. D-Wave: Truth finally starts to emerge. <http://www.scottaaronson.com/blog/?p=1400>, 2013.
- [2] D. Aharonov, M. Ben-Or, and E. Eban. Interactive proofs for quantum computation. In *Proceedings of Innovations of Computer Science*, pages 453–469, 2010.
- [3] B. Altshuler, H. Krovi, and J. Roland. Anderson localization casts clouds over adiabatic quantum optimization. *Proceedings of the National Academy of Sciences of the United States of America*, 107(28):12446–12450, 2010.
- [4] J. Barrett, L. Hardy, and A. Kent. No signalling and quantum key distribution. *Physical Review Letters*, 95(010503), 2005.
- [5] S. Barz, J. F. Fitzsimons, E. Kashefi, and P. Walther. Experimental verification of quantum computation. *Nature Physics*, 9:727–731, 2013.
- [6] S. Boixo, T. Albash, F. M. Spedalieri, N. Chancellor, and D. A. Lidar. Experimental signature of programmable quantum annealing. *Nature Communications*, 4:2067, 2012.
- [7] S. Boixo, T. F. Rønnow, S. V. Isakov, Z. Wang, D. Wecker, D. A. Lidar, J. M. Martinis, and M. Troyer. Quantum annealing with more than one hundred qubits. E-print arXiv:1304.4595. <http://arxiv.org/pdf/1304.4595v2.pdf> (An updated version will appear in [8]), 2013.
- [8] S. Boixo, T. F. Rønnow, S. V. Isakov, Z. Wang, D. Wecker, D. A. Lidar, J. M. Martinis, and M. Troyer. Evidence for quantum annealing with more than one hundred qubits. *Nature Physics*, in press, 2014.

- [9] A. Broadbent, J. F. Fitzsimons, and E. Kashefi. Universal blind quantum computation. In *Proceedings of the 50th Annual IEEE Symposium on Foundations of Computer Science*, pages 517–526, 2009.
- [10] F. E. Browder. On continuity of fixed points under deformations of continuous mappings. *Summa Brasil Math*, 4:183–191, 1960.
- [11] F. Chung. *Spectral Graph Theory*. American Mathematical Society, 1992.
- [12] N. G. Dickson et al. Thermally assisted quantum annealing of a 16-qubit problem. *Nature Communications*, 4:1903, 2013.
- [13] E. Farhi, J. Goldstone, S. Gutmann, and M. Sipser. Quantum computation by adiabatic evolution. E-print arXiv:quant-ph/0001106. <http://arxiv.org/pdf/quant-ph/0001106v1.pdf>, 2000.
- [14] J. F. Fitzsimons and E. Kashefi. Unconditionally verifiable blind computation. E-print arXiv:1203.5217. <http://arxiv.org/pdf/1203.5217v2>, 2012.
- [15] N. Jones. Google and NASA snap up quantum computer D-Wave Two. <http://www.scientificamerican.com/article.cfm?id=google-nasa-snap-up-quantum-computer-dwave-two>, 2013.
- [16] C. C. McGeoch and C. Wang. Experimental evaluation of an adiabatic quantum system for combinatorial optimization. In *Proceedings of the 2013 ACM Conference on Computing Frontiers*, 2013.
- [17] S. Pironio et al. Random numbers certified by Bell’s theorem. *Nature*, 464:1021–1024, 2010.
- [18] B. W. Reichardt, F. Unger, and U. Vazirani. Classical command of quantum systems. *Nature*, 496:456–460, 2013.
- [19] T. F. Rønnow, Z. Wang, J. Job, S. Boixo, S. V. Isakov, D. Wecker, J. M. Martinis, D. A. Lidar, and M. Troyer. Defining and detecting quantum speedup. E-print arXiv:1401.2910. <http://arxiv.org/pdf/1401.2910v1.pdf>, 2014.
- [20] R. Saket. A PTAS for the classical Ising spin glass problem on the Chimera graph structure. E-print arXiv:1306.6943. <http://arxiv.org/pdf/1306.6943v2>, 2013.
- [21] H. Schirmer. Fixed point sets of homotopies. *Pacific Journal of Mathematics*, 108(1):191–202, 1983.
- [22] A. Selby. D-Wave: comment on comparison with classical computers. <http://www.archduke.org/stuff/d-wave-comment-on-comparison/>, 2013.
- [23] J. A. Smolin and G. Smith. Classical signature of quantum annealing. E-print arXiv:1305.4904. <http://arxiv.org/pdf/1305.4904v1.pdf>, 2013.
- [24] M. Troyer. Personal communication, 2014.
- [25] W. van Dam, M. Mosca, and U. Vazirani. How powerful is adiabatic quantum computation? E-print arXiv:0206003. <http://arxiv.org/pdf/quant-ph/0206003v1>, 2002.

- [26] U. V. Vazirani and T. Vidick. Certifiable quantum dice - or, exponential randomness expansion. In *ACM Symposium on Theory of Computing*, 2012.
- [27] U. V. Vazirani and T. Vidick. Fully device-independent quantum key distribution. In *The 5th Innovations in Theoretical Computer Science*, 2014.
- [28] L. Wang, T. F. Rønnow, S. Boixo, S. V. Isakov, Z. Wang, D. Wecker, D. A. Lidar, J. M. Martinis, and M. Troyer. Comment on: “classical signature of quantum annealing”. E-print arXiv:1305.5837. <http://arxiv.org/pdf/1305.5837v1.pdf>, 2013.